Single Cycle Velocity Vector Estimation using a Full-Coherent MIMO Radar Network

Sergio López Fernández#, A. Chaminda J. Samarasekera#, Reinhard Feger#, Andreas Stelzer#, Anusha Hanumegowda$

#Johannes Kepler University Linz, Austria

$ZF Friedrichshafen AG, Germany

{sergio.lopez_fernandez, andawattage.samarasekera, reinhard.feger, andreas.stelzer}@jku.at, anusha.hanumegowda@zf.com

***Abstract*— This work presents a method for estimating the velocity vector of targets in automotive radar applications using a single range-Doppler frame. Our approach leverages the spatial diversity of a full-coherent multiple-input multiple-output system, utilizing both quasi-monostatic and bistatic responses for a more robust and accurate estimation of both the magnitude and direction of the velocity vector. In comparison to traditional methods that rely solely on quasi-monostatic responses, our approach demonstrates superior performance and stability. We present experimental results that validate the effectiveness of our proposed method.**

***Keywords*— Frequency-modulated continuous-wave (FMCW) radar, millimetre wave radar, multi-static radar, MIMO.**

I. Introduction

In automotive applications, frequency-modulated continuous-wave (FMCW) radar is commonly used for velocity estimation. Velocity estimation is based on the principle of the Doppler effect, which is the change in frequency of a wave due to the motion of the transmitter or target. Velocity estimation is typically performed by processing multiple FMCW chirps in a row, using a method such as a two dimensional fast fourier transform (2D-FFT) applied to the received data. This provides range and velocity information about the targets in front of the radar. However, it is important to note that this process only provides an estimate of the radial component of the targets' velocity in the scene and not its movement direction. In conventional approaches the direction of movement can only be estimated over multiple range-Doppler measurements by means of a tracker.

The objective of this work is to propose a method that enables the estimation of both the magnitude and direction of the velocity vector of targets using a multiple-input multiple-output (MIMO) full-coherent FMCW radar network for automotive applications. The proposed method adapts previous techniques [1], [2] exploiting the network's spatial diversity and innovates by using both the quasi-monostatic and bistatic responses. The method requires the target to be detected in at least two of the available responses for each measurement cycle. Additionally, it is independent of the modules' positions and incorporates a clustering process to enhance the estimation's reliability. Also, having access to both quasi-monostatic and bistatic responses provides a more robust approach to target detection by reducing the likelihood of false positives or missed detections [3].

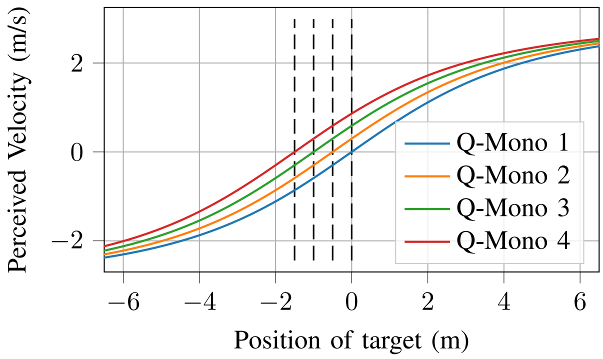

Fig. 1. Perceived velocities of a target moving parallel to four radar modules positioned in a row, measured from their monostatic responses. Target is 5 m apart from the modules, and it moves at 3 m/s from left to right.

Advancements in FMCW radar technology, including improved signal processing and machine learning algorithms, have enabled even more accurate and reliable velocity estimation in real-world driving conditions. The proposed method can further improve the accuracy of velocity estimation by fast estimation of the velocity vector of objects within each range-Doppler cycle, and potentially enhance safety for vulnerable road users especially in the blind spot regions.

Section II describes the method proposed and its basis. In Section III we include a description of the measurement setup: a full cooperative network of four radar modules. Section IV covers the experimental results in 2 different scenarios, with perpendicular and oblique movement. Finally, conclusions are presented in Section V.

II. Proposed Method

As previously introduced, this method utilizes the spatial diversity of a full-coherent radar network. When Doppler processing is performed, each module in the network provides a different radial velocity measurement. This difference in measurement is influenced by several factors, such as the spacing between the modules, their relative positions, the distance to the target, and its trajectory.

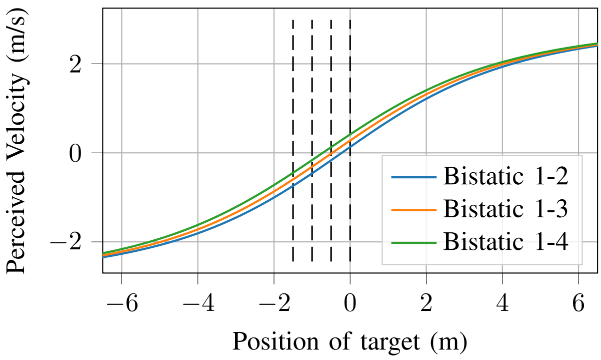

Fig. 2. Perceived velocities of a target moving parallel to four radar modules positioned in a row, measured from the bistatic responses received at the rightmost module. Target is 5 meters apart from the modules, and it moves at 3 m/s from left right.

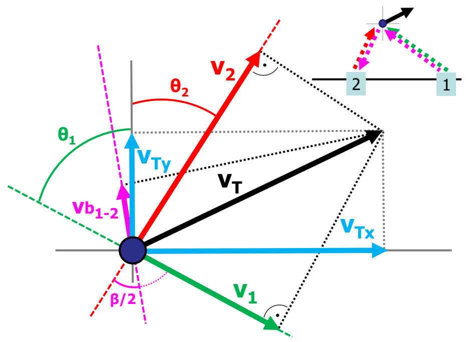

Fig. 3. Target moving with velocity vector $\boldsymbol{v}_{\mathrm{T}}$. The perceived velocity from the qusi-monostatic response of two stations $\boldsymbol{v}_1$ and $\boldsymbol{v}_2$ as well as the bistatic response $\boldsymbol{v}_{b_{1-2}}$ is shown as well as the angle relations between the four.

As a way of illustrating this, Fig. 1 and Fig. 2 show a simulation of the estimated radial velocity evolution for the quasi-monostatic and bistatic responses (for one of the modules) using four different radar modules separated by 0.5 m. The modules are positioned in a row, with dashed lines indicating their respective locations relative to the target. The rightmost module is labeled as module 1. The target is located 5 m away from the row and moves parallel to it at a speed of 3 m/s from left to right. The sign of the perceived velocity indicates the direction of the target, with negative values indicating the target is approaching and positive values indicating it is moving away. The results show that the perceived velocity approaches the true velocity of the target as the distance between the target and the radar modules increases. Our goal is to exploit the difference between these curves to estimate the real velocity of the target and its direction.

To present the method, we will focus on the simplest case where the network is composed of only two modules. Fig. 3 illustrates this situation, where $\boldsymbol{v}_{\mathrm{T}}$ represents the actual velocity of the target and $\boldsymbol{v}_1$ and $\boldsymbol{v}_2$ represent the perceived velocities by each module. These perceived velocities are the result of the quasi-monostatic response. Additionally, Fig. 3 includes $\boldsymbol{v}_{b_{1-2}}$, which is the perceived velocity through the bistatic response. It can be observed that $\boldsymbol{v}_1$ and $\boldsymbol{v}_2$ are the projections of $\boldsymbol{v}_{\mathrm{T}}$ onto the look direction of each module, while $\boldsymbol{v}_{b_{1-2}}$ is the projection onto the bisector of the bistatic angle ($\beta/2$). Through Doppler processing and estimation we have access to $\boldsymbol{v}_1$, $\boldsymbol{v}_2$ and, $\boldsymbol{v}_{b_{1-2}}$. Also, through digital beamforming (DBF) we can estimate both θ_1 and θ_2 - the direction of arrival for each module.

The scalar projection of a vector is the length of the projection of the vector onto a given line or direction. It is also called the scalar component or the magnitude component. The scalar projection is a scalar value. The scalar projection of $\boldsymbol{v}_{\mathrm{T}}$ over the look direction of module n is

$$\left\| \boldsymbol{P}_{\boldsymbol{v}_n}^{\boldsymbol{v}_{\mathrm{T}}} \right\| = \frac{|\boldsymbol{v}_{\mathrm{T}} \cdot \boldsymbol{v}_n|}{\|\boldsymbol{v}_n\|} \tag{1}$$

Following Fig. 3, we can interpret $\left\| \boldsymbol{P}_{\boldsymbol{v}_n}^{\boldsymbol{v}_{\mathrm{T}}} \right\|$ as the module of any of the perceived velocities ($\|\boldsymbol{v}_n\|$), if we simplify and decompose the scalar product we can express the relation between $\boldsymbol{v}_{\mathrm{T}}$ and $\boldsymbol{v}_n$ as

$$V_n^2 = V_{\mathrm{T}_x} \cdot V_{n_x} + V_{\mathrm{T}_y} \cdot V_{n_y} \tag{2}$$

where V_{T_x} and V_{T_y} are the Cartesian components of $\boldsymbol{v}_{\mathrm{T}}$ taking the target as origin as shown in Fig. 3. V_{n_x} and V_{n_y} are the components of $\boldsymbol{v}_n$ and V_n its module. Then, with access to at least two different modules we can construct a system of linear equations and estimate a value for V_{T_x} and V_{T_y}. For the system to have a solution the two estimated radial velocities must be linearly independent. This depends on the separation between modules and how far the target is.

In this work, in comparison to [2], we are using a full-coherent MIMO network consisting of four different radars to increase the robustness of our target estimation. This configuration provides us with ten different sets of data, including four quasi-monostatic responses and six different bistatic paths. Access to the bistatic responses improves the performance of the network [3], providing stability and robustness to the process. Also as a result, we have more equations than variables, making the system overdetermined, which is beneficial for improving the accuracy of the estimation and reducing the impact of noise and errors.

To estimate the target's velocity we need at least information from two different responses. To solve the overdetermined system when we have access to more we are using a least-squares approach, which involves minimizing the sum of the squared errors between the observed data and the predicted data based on the model. If any response is missing data due to missed detections or similar effects it will not be considered. Furthermore, as an extra step for stability, we have implemented a modified version of DBSCAN as described in [4] to improve the target detection, grouping and, successful extraction of the parameters. This method allows us to estimate both the velocity and direction of the target accurately. Additionally, it is possible to perform the estimation for each measurement cycle individually. Moreover, this can be achieved independently of the module positions.

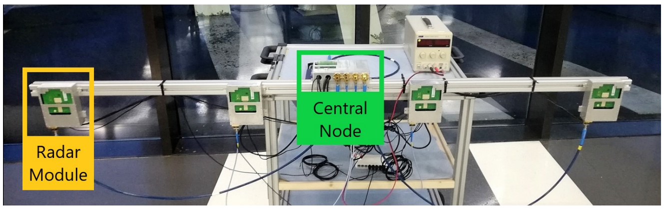

Fig. 4. Network setup. The central node is fixed in the middle with the other four modules on a line 0.5 m apart form each other, two on each side.

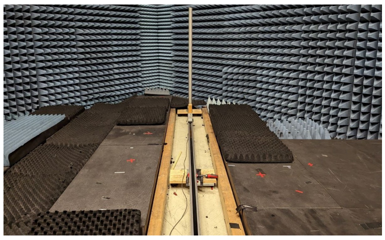

Fig. 5. First measurement setup: The target is affixed to the rail, enabling perpendicular movement relative to the radar network. The image provides the perspective of the radar network.

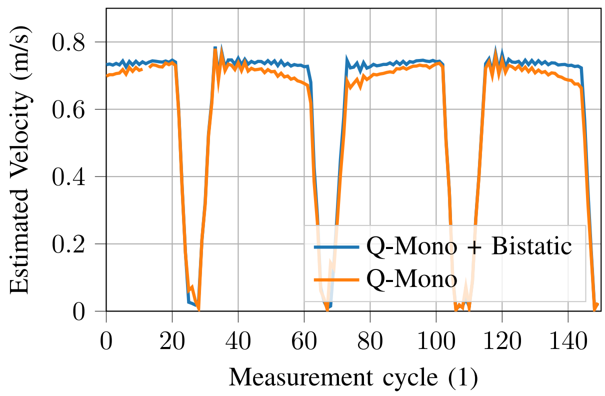

Fig. 6. Estimated magnitude of the velocity vector for the target for the first scenario. It can be seen how the use of the bistatic information improves the accuracy of the estimation. Moreover, it avoids miss detections.

III. Data Measurement Setup

The radar network used to conduct the measurements is similar to the one described in [3]. It consists of 5 individual modules in a star configuration with the central node serving as a master for the network. For the network to work coherently, the master module generates a sequence of FMCW chirps, ranging from 38 to 40.5 GHz, which are transmitted to the other four modules via coaxial cables. The modules then up-convert the chirps to 76-81 GHz for transmission. In addition, the master module transmits a reference clock signal, an analogue-to-digital converter (ADC) synchronization signal, and a ramp synchronization signal. This ensures that all four modules work with the same reference clock and that their ADCs are synchronized, allowing for simultaneous transmission by all four modules. As a main difference to [3], in this case the five modules are mounted on a line on a cart separated 0.5 m from each other as shown in Figure 4. In these measurements, all 12 TX antennas will be utilized to transmit the FMCW signal, while all 16 RX antennas will be used to collect information. The setup employs a Doppler modulation, as described in [5] and [6], which enables the separation of the 192 MIMO channels. The start frequency is 76.5 GHz with a 900 MHz bandwidth, we will use 512 IF samples with a chirp time of 32 μs.

IV. Experimental Results

Our study aimed to investigate the performance of the proposed method estimating the velocity vector of a target in two different scenarios. We conducted measurements for each scenario using a metal pole attached to a rail system in an anechoic chamber. The pole measured 125 cm in length and was programmed to move at a constant speed of 0.75 m/s along the rail. For each scenario, we transmitted and collected 256 FMCW chirps per cycle, and performed 150 cycles of measurements. The measurements were conducted in an anechoic chamber. The first scenario involved the pole moving in a straight line perpendicular to the network, while the second scenario involved the pole in an oblique orientation.

A. *Perpendicular Movement*

For the first scenario the radar network was situated perpendicular to the rail to which the pole was fixed. Fig. 5 shows the setup in the anechoic chamber. To estimate the velocity vector, we employed two different input configurations. In the first configuration, we made the simplest assumption possible, which involved using only two independent radars. As a result, we utilized the quasi-monostatic information from the modules located at the extremes of the network. In the second configuration, we fully leveraged the network's capabilities by incorporating all quasi-monostatic and bi-static responses. The results for the module of the velocity vector are shown in Fig. 6. The graph reveals distinct plateaus and valleys that correspond to the pole's backward and forward motion along the rail, as well as its halts at either end. Notably, the inclusion of bistatic information has enhanced the estimation process, as evidenced by the complete coverage of the measurement range without gaps (such as the one observed around the 12th cycle), and a more accurate velocity value. The root-mean-square error (RMSE) of the magnitude estimation improves up to 0.017 m/s from the 0.043 m/s in the quasi-monostatic case.

Fig. 7 depicts the estimated direction of the velocity vector for two distinct measurement cycles, as well as the positions of the pole and the four modules for reference. Furthermore, location estimations for all 150 measurement cycles are provided.

B. *Oblique Movement*

In the second scenario, the radar network was placed at an oblique angle to the rail. Figure 8 illustrates the configuration of the setup in the anechoic chamber.

Similar to the first scenario, we analysed the available data in two separate configurations. The first configuration utilized quasi-monostatic information solely from the modules

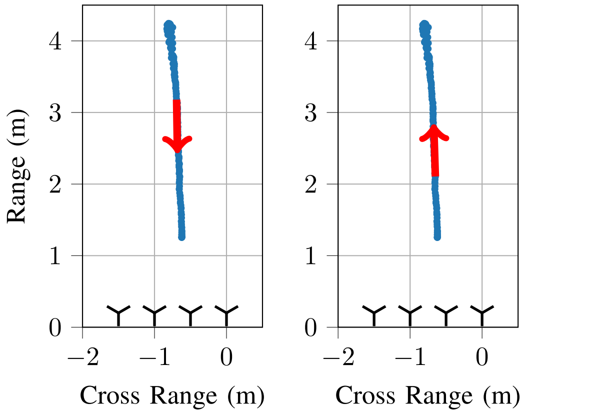

Fig. 7. Comparing velocity vector direction estimates from two measurement cycles for a target moving perpendicularly to the network. The position of the pole (estimated using range information and DBF) is denoted by blue dots in all cycles, with the four modules positions provided for reference.

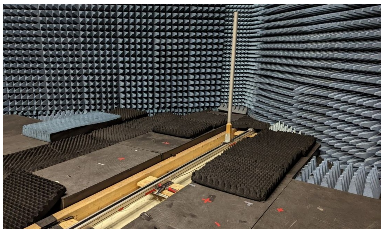

Fig. 8. Second measurement setup: The target is affixed to the rail, enabling oblique movement relative to the radar network. The image provides the perspective of the radar network.

on both extremes, while the second configuration included all quasi-monostatic and bistatic responses. Fig. 9 illustrates the magnitude of the velocity vector for both cases.

Like in Fig. 6, the bistatic processing effectively eliminates any gaps in measurements that arise due to the limited field of view in the quasi-monostatic setup. Also, the RMSE improves to 0.045 m/s from the 0.049 m/s in the quasi-monostatic case. Fig. 10 depicts the estimated direction for the velocity vector in two different measurement cycles. The position of the pole for the whole measurement and the four modules has been added

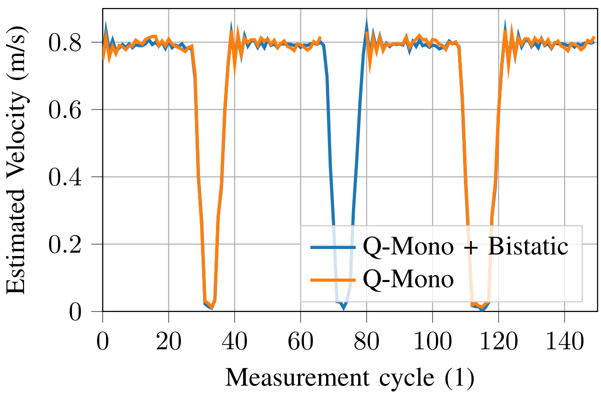

Fig. 9. Estimated magnitude of the velocity vector for the target for the second scenario. It can be seen how the use of the bistatic information allows the estimation to be performed for each measurement cycle.

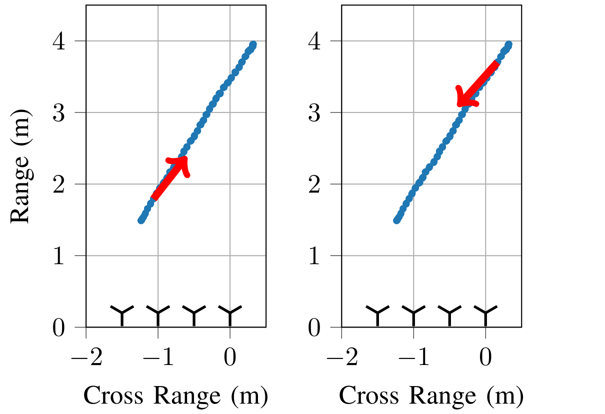

Fig. 10. Comparing velocity vector direction estimates from two measurement cycles for a target moving obliquely to the network.The position of the pole (estimated using range information and DBF) is denoted by blue dots in all cycles, with the four modules positions provided for reference.

for reference. However, it is important to note that these results highlight the necessity of an additional layer of processing to evaluate the quality of responses before integrating them into the estimation process. Discriminating noisier responses can further enhance the accuracy of the estimation by leveraging the additional information provided by the bistatic responses.

V. Conclusion

This paper proposes an approach for estimating velocity vectors using the scalar projection of vectors principle. The method leverages quasi-monostatic and bistatic data from multiple stations, working coherently to achieve a stable estimation of target velocity. By analysing the differences in radial velocities perceived by each station, the approach accurately estimates both velocity and direction. The method can deliver independent results for each measurement cycle, while also remaining highly flexible in terms of its physical configuration, since it is independent of module position.

References

[1] V. S. Chernyak, *Fundamentals of Multisite Radar Systems: Multistatic Radars and Multiradar Systems 1st ed.* Gordon and Breach Science Publishers, 1998.

[2] B. Nuss, Y. L. Sit, and T. Zwick, "3D radar image fusion using OFDM-based MIMO radar," in *Proc. German Microwave Conference*, pp. 209–212, 2016.

[3] S. L. Fernández, A. C. J. Samarasekera, R. Feger, and A. Stelzer, "Measurement-Based Analysis of a Non-Coherent MIMO Radar Network for Automotive Applications," in *Proc. 19th European Radar Conference*, pp. 1–4, 2022.

[4] T. Wagner, R. Feger, and A. Stelzer, "Modification of DBSCAN and application to range/Doppler/DoA measurements for pedestrian recognition with an automotive radar system," in *Proc. European Radar Conference*, pp. 269–272, 2015.

[5] N. Touati, C. Sturm, M. Imran, A. Vanaev, M. Kohler, K. Krupinski, W. Malik, and U. Lübbert, "High Angle Resolution Automotive Radar Based on Simultaneous 12Tx Doppler-Multiplex MIMO," in *Proc. 17th European Radar Conference*, pp. 386–389, 2021.

[6] C. Sturm, Y. L. Sit, G. Li, H. A. Vayghan, and U. Lübbert, "Automotive Fast-Chirp MIMO Radar with Simultaneous Transmission in a Doppler-Multiplex," in *Proc. 19th International Radar Symposium*, pp. 1–6, 2018.